RSC Advances

ROYAL SOCIETY OF CHEMISTRY

www.rsc.org/advances

Graphical Abstract

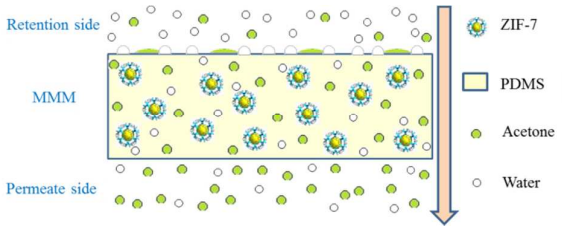

Mixed matrix membrane containing ZIF-7 exhibits the excellent performance in the recovery of acetone from fermentation broths.

RSC Advances

RSCPublishing

ARTICLE

Recovery of Acetone from Aqueous Solution by ZIF-7/PDMS Mixed Matrix Membranes

Cite this: DOI: 10.1039/xoxxoooooox

Yunpan Ying, Yuanlong Xiao, Jing Ma, Xiangyu Guo, Hongliang Huang, Qingyuan Yang, Dahuan Liu *, Chongli Zhong *

Received ooth January 2012,
Accepted ooth January 2012

DOI: 10.1039/xoxxoooooox

www.rsc.org/

Metal-organic frameworks (MOFs) have exhibited promising applications in gas and liquid separation. As a subclass of MOFs, zeolitic imidazolate frameworks (ZIFs) are attracting more and more interests because of their unique thermal and chemical stability. One of representative ZIFs, ZIF-7, has super-hydrophobic pore, making it a perfect filler in polymer membrane for recovering acetone from fermentation broths. In this study, mixed matrix membranes (MMMs) based on ZIF-7 and polydimethylsiloxane (PDMS) were prepared, which display improved acetone-water total flux and separation factor simultaneously compared with pure PDMS membrane. The separation factor can reach up to 39.1 with high flux of 1236.8 $g \cdot m^{-2} \cdot h^{-1}$ at 333 K, which is the highest value among the reported ones up to now to the best of our knowledge.

1. Introduction

As one of important petrochemical products and commonly used organic solvents, acetone can be acquired by chemical synthesis and fermentation production of agricultural products such as acetone-butanol-ethanol (ABE) fermentation broth. Up to now, a great deal of research efforts were devoted to recovering butanol or ethanol, whereas those for acetone are very scare, which is also of significant importance from both economic and environmental points of view[1]. In general, the concentration of acetone in fermentation broth is very low (below 2 wt. %), indicating that the operation cost should be high if the conventional recovering methods are used, such as distillation and liquid-liquid extraction. In contrast, pervaporation (PV) is attracting more and more widespread concern due to its high efficiency and low energy consumption, especially for low concentration liquid separation[2,3]. PV process has been widely used in the dehydration process of organic solvent-water mixtures[4,5], the removal/recovery of organics from aqueous solution[6,7] and the separation of organic mixtures[8,9]. Based on solution-diffusion mechanism[3], the PV membrane technology was developed, where the functional membrane is the key for a certain purpose of separation[10,11]. Thus, great efforts are being made in the development of such membranes with excellent performance. Mixed matrix membranes (MMMs), originally constructed from filler and polymer matrix, were considered as the most promising ones[12-17]. These membranes combine the easy processibility and low cost of polymer as well as the high intrinsic permeability or selectivity of the fillers[18]. Despite the advantages of MMMs in liquid PV, the separation performance of such membranes still needs to be further improved to meet the practical demands. In this respect, MMMs based on metal-organic frameworks (MOFs) provide a good platform thanks to the highly designable structure and chemical diversity of MOFs[19-24]. These kinds of MMMs have actually displayed good performance in gas separations[25-31]. However, for liquid separation, only very limited works were reported up to now[14-17, 32-34]. These works have suggested that MMMs are very promising in the recovery of organic compounds, while the investigations on acetone are very scare.

Therefore, in this work MMMs with ZIF-7 and polydimethylsiloxane (PDMS) were prepared for the recovery of acetone from aqueous solution. As a typical one of zeolitic imidazolate frameworks (ZIFs), a subclass of MOFs, ZIF-7 is constructed by connecting zinc cluster to benzimidazolate (bIM) ligand in sodalite (SOD) topology structure (Fig. 1(a)) with high stability[35]. More importantly, ZIF-7 has the hexagonal window size of 0.29 nm in the cage with super-hydrophobicity[36,37], which makes it ideal candidate filler in polymers for recovering organics, such as acetone. Polydimethylsiloxane (PDMS) was selected as the polymer matrix because of its superior structure and properties. It is a kind of organic permselective membrane material with perfect comprehensive performance, with high selectivity and good biocompatibility for volatile organic compounds (VOCs) in solution. Bearing this in mind, it is expected that the as-

synthesized MMMs may efficiently separate acetone from aqueous solution.

2. Experimental

2.1 Materials

Zinc nitrate hexahydrate (Zn $(NO_3)_2 \cdot 6H_2O$, >99%) and bIM (>99%) were purchased from Aladdin. PDMS (A.R., $\overline{Mw} = 10{,}000$) was supplied by Shandong Zhaoyang Chemical Company. Polyvinylidene-fluoride film supports (PVDF, pore size = 0.22 μm) were purchased from Beihua Liming Membrane Separation Technology Co. Ltd. *N, N'*-dimethylformamide (DMF, >99%), n-heptane (A.R.), methanol (A.R.), acetone (A.R.) were purchased from Beijing Chemical Works. Tetraethyl- orthosilicate (TEOS, A.R.) as the cross-linker was purchased from Xilong Chemical Co., Ltd. Dibutyltin dilaurate (DBTDL, A.R.) as the catalyst was purchased from Tianjin FuChen Chemical Reagents Factory. All the chemicals were used as received without further purification.

2.2 Synthesis of ZIF-7

ZIF-7 was synthesized by a modified recipe reported by Li et al. at 298.15 K[38]. 300 mL DMF was added to a solid mixture of 0.906 g Zn $(NO_3)_2 \cdot 6H_2O$ and 2.307 g bIM with stirring (molar composition of the synthesis solution of Zn^{2+}/bIM/DMF = 0.154/1/200) for 48 h, followed by the separation of product using a centrifuge. Then the solid was washed with MeOH for five times (100ml ×5) to remove unreacted reagents and DMF within ZIF-7 pores by stirring overnight. After centrifugation, the particles are directly dispersed into the H_2O/EtOH (weight ratio is 30/70) mixture. The particle agglomeration can be avoided using such kind of solvent mixture, as suggested in literatures[39, 40]. The sample was kept in vacuum oven at 333 K overnight for the following study.

2.3 Membranes preparation

The n-heptane solution of ZIF-7 was prepared by adding a certain weight of grinded ZIF-7(about 80 nm in size as shown in Fig. 3(a)) to n-heptane (1.0 g). The solution was stirred for 6 hours, accompanying with sonication for 15 min every hour. Then, PDMS was added into the mixture with the total weight of ZIF-7 and PDMS was 1.5 g (the concentration of ZIF-7/PDMS in n-heptane is 0.6 $g \cdot g^{-1}$). Subsequently, the solutions of different weight ratio were stirred for 4h accompanying with sonication for 15 min every hour. TEOS and DBTDL were then added and the weight ratio of PDMS: TEOS: DBTDL was kept as 10:1:0.1. PDMS homogeneous casting solution contained 0, 5, 10, 15, 20, 25, 30, 35, 40 wt. % ZIF-7 nanocrystals were prepared. PVDF film was used as the support with an easy processing procedure. The PVDF support was immersed into a 10 wt. % ethanol aqueous solution and then into deionized water for 10 min successively. Subsequently, the wet PVDF support was fixed on the glass plate with adhesive tape. To remove the excess deionized water, the PVDF support was simply wiped by filter paper[41]. The solution was dropped on the pre-treated wet PVDF support and casted with the casting machine. The solvent was evaporated for 4 h at 298 K and then transferred into vacuum oven for 8 h at 353 K. In this way, PV experiments were conducted using these membranes. The samples prepared on plastic petri dish were used in uptake experiment and XRD characterization of membranes.

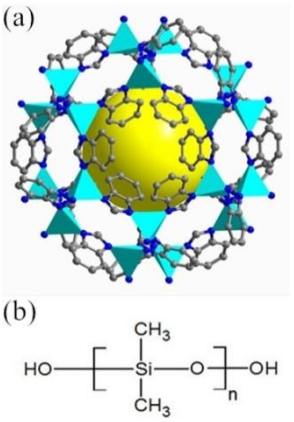

Fig.1 Chemical structures of (a) ZIF-7 (Zn: cyan tetrahedral; C: gray; N: blue; H atoms in bIM linkers were omitted for clarity) and (b) PDMS.

2.4 Characterization

X-ray diffractometry (XRD) analysis of ZIF-7 nanocrystals and MMMs was conducted on a SHIMADZU XRD-6000 X-ray diffractometer in reflection mode using Cu Kα radiation (λ = 1.5406 Å) at 298 K. The 2θ range from 5° to 50° was scanned with a step size of 0.05 °. The morphologies of ZIF-7 and the membranes were characterized by scanning electron microscopy (SEM) (FEI, JEOL JSM-7800F microscope). To get sharp clear cross-sectional images of the membranes, the samples were fractured under liquid nitrogen. All samples were mounted on tape and coated with a 1.5–2 nm Au layer to increase the conductivity and the measurements were operated under 10-20 kV acceleration voltage[42]. The ATR-FTIR (attenuated total reflection Fourier transform infrared spectroscopy) characterization was performed on Nicolet 6700 FTIR spectrophotometer. Spectra were recorded in the 4000-650 cm^{-1} wave number range. The contact angle of the membranes was measured using a DSA 100 system. CO_2 adsorption isotherm of ZIF-7 powder at 298K was measured on an Autosorb-iQ-MP (Quantachrome Instruments) automated gas sorption analyser. Before measurements, the samples were degassed at 423 K overnight.

2.5 Uptake experiment

Uptake experiments of PDMS membrane and MMMs were performed at 303 K. Before the uptake experiment, the membrane sample was dried at 353 K for 3 h and weighed (denoted by W_D, g). Then, the membrane was immersed in 1 wt. % acetone solution for 22 h, and after that it was wiped with tissue paper and weighed again (denoted by W_W, g). The uptake (wt. %) was calculated according to[33, 43-46]

$$Uptake(\text{wt.}\%) = \frac{W_W - W_D}{W_D} \times 100\% \quad (1)$$

where W_D and W_W are masses (g) of a dry and a swollen membrane, respectively.

2.6 Pervaporation

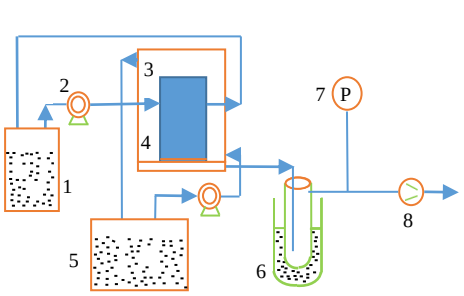

1. feed tank
2. peristaltic pump
3. membrane module
4. membrane
5. water bath
6. cold trap
7. vacuum gauge
8. vacuum pump

Fig. 2 Schematic diagram of PV experiment.

PV experiments were performed in a home-made device (Fig.2). The prepared membrane was supported by a porous sintered stainless steel on the permeate side of membrane cell. The effective area of PV cell was 20.0 cm^2. The feed liquid in the feed tank was cycled and has a volume of 2.5 L to ensure the weight concentration is constant during the PV process. The water bath was also cyclic and used to ensure the PV was conducted at a certain and stable temperature. The permeate vapor was collected by a condenser pipe immersed in liquid nitrogen. The pressure of the permeate side was kept below 500 Pa by vacuum pump and was monitored by a digital vacuum gauge. Each PV experiment of membrane was conducted for a certain time after being stabilized at least 2 h. The flux was calculated by condensing and freezing the permeate vapor in the condenser pipe. Moreover, at least three identical membranes were tested for each of the PV condition to ensure the reliability of the results. The frozen permeate was heated up to 298 K and then weighted to calculate the flux. The concentration was analyzed by using a gas chromatography (GC, Agilent Technologies Inc.). Total flux and separation factor were calculated through the following equations:

$$J = \frac{m}{A \cdot t} \quad (2)$$

and

$$\alpha = \frac{Y_{Acetone}/(1 - Y_{Acetone})}{X_{Acetone}/(1 - X_{Acetone})} \quad (3)$$

where J is the total flux ($g \cdot m^{-2} \cdot h^{-1}$), m is the mass of the collected permeate sample (g), A is the effective membrane area (m^2), t is the collecting sample time (h), α is the separation factor of acetone-water mixture, $Y_{Acetone}$ and $X_{Acetone}$ are the weight concentration of acetone in the permeate and the feed respectively(wt.%).

3. Results and Discussion

3.1 Characterization

The morphology of ZIF-7 nanocrystals prepared in DMF at 298 K is shown in Fig. 3(a). According to the SEM image, ZIF-7 has a uniform particle size distribution of 80 nm. It should be noted that the agglomeration of nanoparticles can be avoided to a certain extent if the samples are dried after being washed in EtOH/H_2O mixture. Cross sectional SEM images of the prepared PDMS membrane and MMMs with different ZIF-7 loadings are shown in Fig. 3(b-f). It can be seen that all of the membranes are dense and defect-free. As illustrated in Figs. 3(c-f), ZIF-7 was homogeneously dispersed and closely embedded in the PDMS phase, with few voids around them observed, indicating that the polymer matrix and ZIF-7 are compatible well. The sizes of ZIF-7 are still about 80 nm similar to that of grinded ZIF-7 (Fig. 3a), indicating that they did not separate during membrane fabrication. However, when the ZIF-7 loading was above 25%, the dispersion of ZIF-7 is not good compared to those in MMMs with 10~25 wt. % filler loading, and there are obvious aggregations of particle surrounded by voids in polymer matrix (Fig. S1 in ESI†).

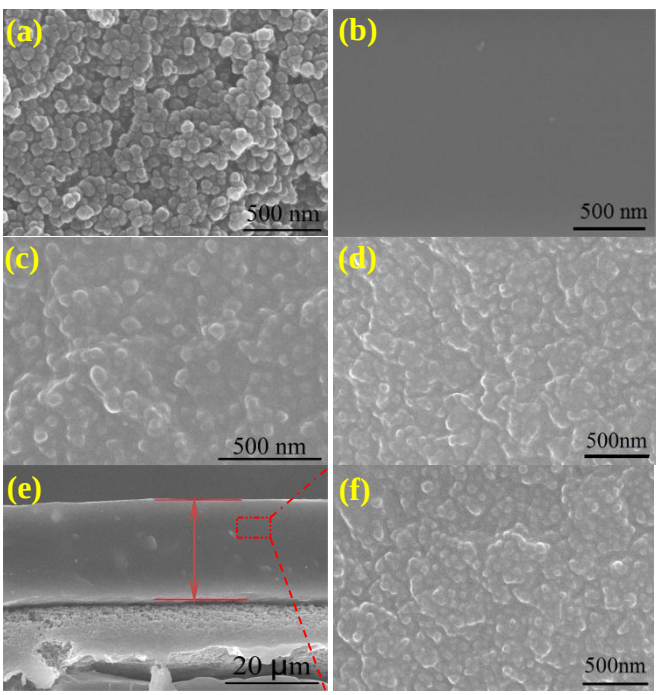

Fig. 3 Top view SEM image of (a) ZIF-7. Cross sectional SEM images of (b) PDMS membrane and (c-f) MMMs with different ZIF-7 loadings (c, 10 wt. %; d, 20 wt. %; e and f, 25 wt. % with different magnifications).

In order to determine the structure of the prepared ZIF-7, the experimental XRD pattern (denoted as ZIF-7-Exp) was conducted to be compared with the simulated XRD pattern (denoted as ZIF-7-Sim). As shown in Fig. 4, they are in good agreement with each other. The PXRD peaks of ZIF-7 can also

be found in the XRD patterns of MMMs, demonstrating that the structure of ZIF-7 remains intact in the polymer matrix. The porous structure of ZIF-7 nanoparticles was investigated through measuring the CO_2 adsorption isotherm as shown in Fig. S2 in the ESI†, since there is no adsorption of N_2 at 77 K due to the small pore diameter[47-49].

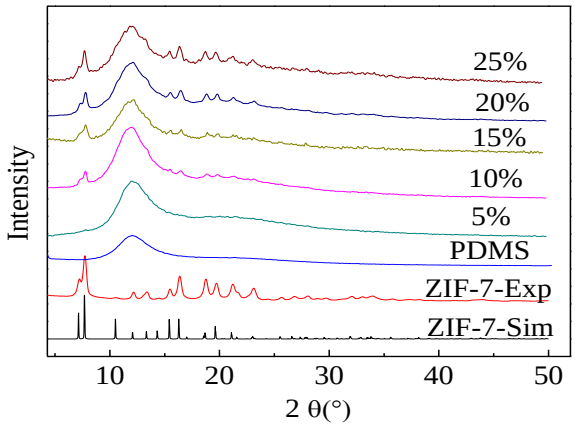

Fig. 4 XRD patterns of ZIF-7 and MMMs with different ZIF-7 loadings.

The FTIR spectra of ZIF-7 and MMMs are shown in Fig. 5. Among these MMMs, two obvious peaks at approximately 1455 and 750 cm^{-1} were observed, which are corresponding to those in ZIF-7 particles identified as C=C and C-H bonds in the benzene functional group of benzimidazole[50]. These results also confirmed that ZIF-7 was successfully incorporated into the MMMs and no chemical reaction was found between ZIF-7 and PDMS.

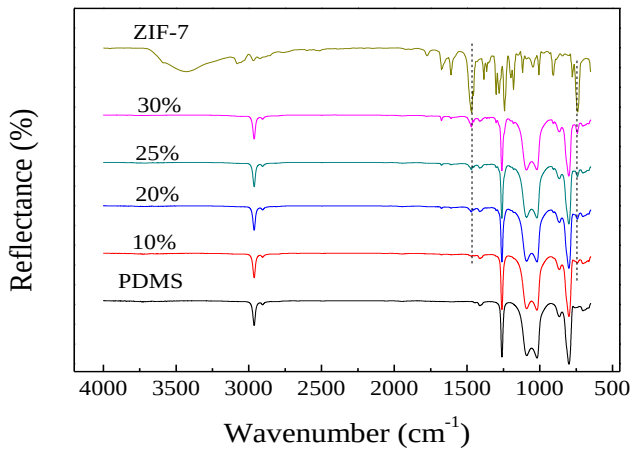

Fig. 5 FTIR spectra of ZIF-7 and MMMs with different ZIF-7 loadings.

3.2 Pervaporation

3.2.1 Effect of ZIF-7 loading The effect of the ZIF-7 loading in MMMs on the PV performance at 333K is shown in Fig. 6. It can be observed that the total PV flux increases with the increase of ZIF-7 loading, from 732.6 $g \cdot m^{-2} \cdot h^{-1}$ for pure PDMS membrane up to 1542.6 $g \cdot m^{-2} \cdot h^{-1}$ for MMMs with 40 wt. % filler. This is attributed to high specific interactions between acetone and the super-hydrophobic ZIF-7 nanocrystals. Besides the super-hydrophobic pores of ZIF-7 providing preferential diffusion paths for acetone, the aggregation at high loadings may form voids that could also contribute to the increase of flux. Moreover, a great enhancement in separation factor is achieved with the help of such super-hydrophobic filler. In fact, the hydrophobicity of MMM also increases with increasing the filler content, as illustrated by the increase of contact angle as shown in Fig. 7. It is attributed to the fact that the amount of ZIF-7 nanocrystals as well as their super-hydrophobic pores exposed to the membrane surface increases with the increase of ZIF-7 loading. The increasing hydrophobicity of MMMs could also play a positive role in the improvement of separation performance. However, separation factor decreases on the condition that the ZIF-7 loading is above 25 wt. %. This may be due to the formation of voids between nanoparticles, which become low selective transport paths[34] (Fig. S1 in ESI†).

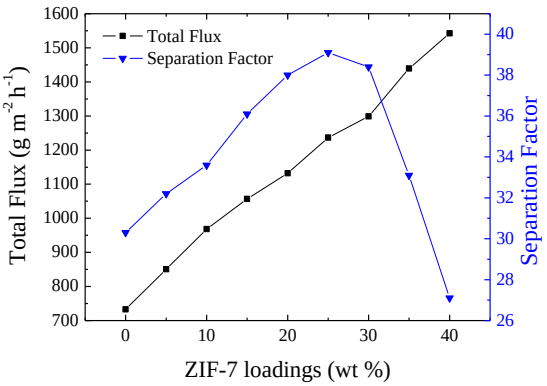

Fig. 6 The effect of ZIF-7 loading on PV performance of MMMs with feed solution of 1 wt. % acetone at 333K.

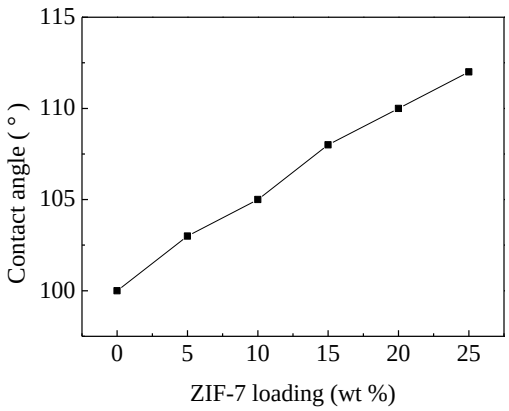

Fig. 7 The contact angle of MMMs with different ZIF-7 loadings.

It is known that PV process follows solution-diffusion transport mechanism, which contains three steps: adsorption,

diffusion, desorption[7]. The PV performance is the comprehensive result of these three steps. Thus, the uptake characteristic of a membrane plays an important role in PV performance since it indirectly reflects the affinity between permeating molecules and membrane[51,52]. The uptake of MMMs increases with increasing filler content, because the presence of super-hydrophobic ZIF-7 nanoparticles can enhance the acetone uptake into the membranes. Since the addition of ZIF-7 changes membrane characteristics of solvent-induced swelling, it will also affect the PV performance. As shown in Fig. 8, the dependence of uptake on ZIF-7 loading is similar to that of the total PV flux (Fig. 6).

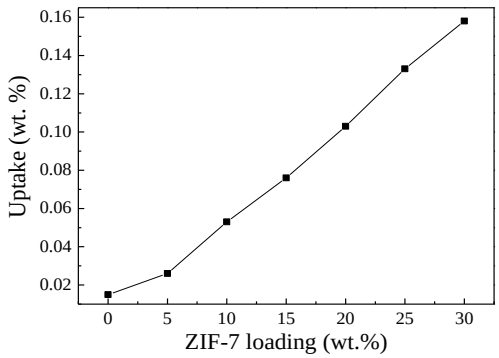

Fig. 8 The average uptake (wt. %) of different ZIF-7 loading MMMs.

3.2.2 Effect of temperature To investigate the effect of temperature, we further conducted PV experiments of PDMS membrane and the MMM with 25 wt.% ZIF-7 loading at different temperatures, including 303 K, 313 K, 323 K and 333 K. As shown in Fig. 9, both the total flux and the separation factor increase as temperature increases. High temperature promotes the pass of both acetone and water through the membrane. However, acetone has lower boiling point (329.4 K) than water, inducing that acetone molecules can pass the membrane easier. Thus, the PV separation performance can be enhanced with the increase of feed temperature. Moreover, according to the solution-diffusion mechanism, the effect of temperature on the total flux can be described by Arrhenius equation:

$$J = J_0 \exp(-\frac{E_a}{RT}) \qquad (4)$$

where J is flux, J_0 is pre-exponential factor, R is universal gas constant, T is the operating temperature, and E_a is the apparent activation energy of flux. Fig. 10 presents the plots of ln (J) versus operation temperature for pristine PDMS and the MMM with 25 wt. % ZIF-7. According to equation (4), E_a of total flux across the MMM is 27.5 kJ·mol^{-1}, showing a 28.7% decrease in energy barrier compared with the pristine PDMS membrane (38.6 kJ·mol^{-1}). Such low energy barrier leads to the less resistance for acetone molecules and water molecules passing the membranes[53]. On the other hand, increasing the feed temperature will lead to the increase of the energy consumption, which is not suitable from the practical point of view. Therefore, the operating temperature should be optimized balancing the separation performance and energy consumption, for example, slightly above the acetone boiling point, 333 K.

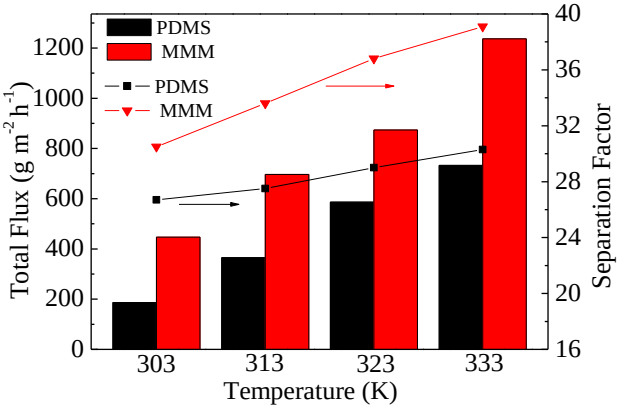

Fig. 9 The effect of PV temperature on PV performance.

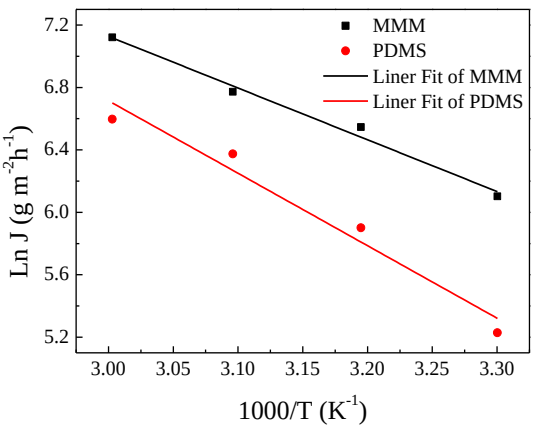

Fig. 10 The effect of PV temperature on the PV total flux.

3.2.3 Effect of feed concentration PV performance of MMMs is also influenced by feed concentration, as shown in Fig. 11. The PV experiments of MMM with 25 wt. % loading were conducted with different feed solutions at 333 K. There is a "trade-off" relationship between total flux and separation factor with the increase of feed concentration. The MMM exhibits higher separation efficiency towards low concentration of acetone aqueous solution, which is ascribed to the fact that the decreased uptake caused by low concentration solution can reduce the free volume. As a result, acetone molecules can pass the membrane more easily than water molecules to induce the increase of separation factor. In addition, with increasing concentration, associated effect between water and acetone becomes more and more significant, resulting in the easy pass of water molecules through membrane[54,55]. Correspondingly, the separation factor decreased from 39.1 to 28.3 with the

concentration of feed solution increases from 1 to 5 wt. %, a decrease of 27.6 %.

3.3 Comparison with other membranes

Table 1 shows a comparison of PV performance of the ZIF-7/PDMS membranes with various membranes previously reported in literatures. To the best of our knowledge, both the total flux and the separation factor of MMM with 25 wt. % ZIF-7 loading at 333 K are higher than all of the reported values. The excellent separation performance of these MMMs for acetone/water mixture is mainly attributed to the super hydrophobicity of the filler ZIF-7 crystals, as well as their well dispersion in the hydrophobic polymer matrix. This superior performance not only demonstrates the potential of incorporating ZIF-7 into PDMS matrix for recovering acetone from low concentration of aqueous solution, such as fermentation broth, but also opens a new way for the fabrication and application of ZIF-7 based MMMs.

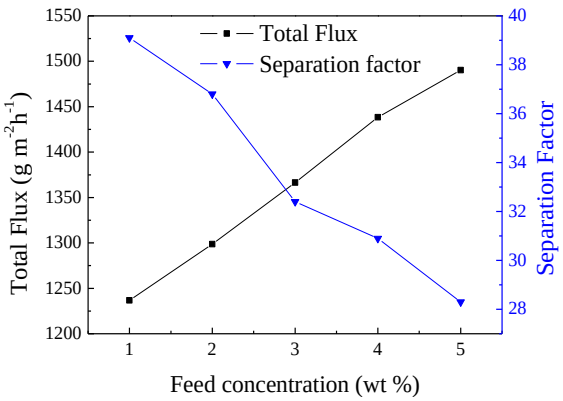

Fig. 11 The effect of feed concentration on PV performance.

Table 1 Comparison with other membranes

Membrane	Temperature (K)	Total flux (g m^{-2} h^{-1})	Separation factor	Ref.
PDMS/ceramic	310.15	-	20.6	6
PERVAP-1060	313.15	340	14.5	56
PERVAP-1070	313.15	100	16.7	56
Silicalite-PDMS	343.15	907	13.7	57
PEBA 2533	296.15	140.1	3.3	58
ZIF-7/PDMS	333.15	1236.8	39.1	This work

Conclusions

Mixed matrix membranes based on super-hydrophobic ZIF-7 and hydrophobic PDMS were prepared and applied in recovering acetone from aqueous solutions. The results show that ZIF-7 were well dispersed in PDMS matrix without obvious defects, and the super hydrophobicity of ZIF-7 enhanced both the total flux and separation factor of the MMMs. Among the MMMs prepared, the one with 25 wt.% ZIF-7 shows better separation performance than all the membranes reported so far for acetone recovery from aqueous solutions. More importantly, this work demonstrates that the addition of MOFs to polymers is a promising way to prepare MMMs that may find industrial applications for recovering organic solvents from aqueous solutions.

Acknowledgements

Financial support by the National Key Basic Research Program of China ("973") (2013CB733503) and the Natural Science Foundation of China (Nos. 21136001 and 21276008) are greatly appreciated.

Notes and references

State Key Laboratory of Organic-Inorganic Composites, Beijing University of Chemical Technology, Beijing 100029, China
E-mail: liudh@mail.buct.edu.cn, zhongcl@mail.buct.edu.cn

† Electronic Supplementary Information (ESI) available: Cross sectional SEM of MMM with 30 wt. % ZIF-7 loading, CO_2 adsorption isotherm of ZIF-7 powder at 298 K. See DOI: 10.1039/b000000x/

1 J. Li, G. Zhang, S. Ji, N. Wang and W. An, *J. Membr. Sci.*, 2012, **415-416**, 745.
2 P. Shao and R. Y. M. Huang, *J. Membr. Sci.*, 2007, **287**, 162.
3 B. Van der Bruggen and P. Luis, *Curr. Opin. Chem. Eng.*, 2014, **4**, 47.
4 D. Hua, Y. K. Ong, Y. Wang, T. Yang and T. Chung, *J. Membr. Sci.*, 2014, **453**, 155.
5 S. Sorribas, P. Gorgojo, C. Tellez, J. Coronas and A. G. Livingston, *J. Am. Chem. Soc.*, 2013, **135**, 15201.
6 G. Liu, W. Wei, H. Wu, X. Dong, M. Jiang and W. Jin, *J. Membr. Sci.*, 2011, **373**, 121.
7 H. Fan, Q. Shi, H. Yan, S. Ji, J. Dong and G. Zhang, *Angew. Chem. Int. Ed.*, 2014, **53**, 5578.
8 X. Dong and Y. S. Lin, *Chem. Commun.*, 2013, **49**, 1196.
9 C. Zhao, N. Wang, L. Wang, H. Huang, R. Zhang, F. Yang, Y. Xie, S. Ji and J. Li, *Chem. Commun.*, 2014, **50**, 13921.
10 J. Zuo, G. M. Shi, S. Wei and T. Chung, *ACS Appl. Mater. Interfaces*, 2014, **6**, 13874.
11 S. Sun, T. Chung, K. Lu and S. Chan, *AIChE J.*, 2014, **60**, 3623.
12 J. Caro, *Curr. Opin. Chem. Eng.*, 2011, **1**, 77.
13 H. Vinh-Thang and S. Kaliaguine, *Chem. Rev.*, 2013, **113**, 4980.
14 S. Liu, G. Liu, J. Shen and W. Jin, *Sep. Purif. Technol.*, 2014, **133**, 40.
15 X. Liu, H. Jin, Y. Li, H. Bux, Z. Hu, Y. Ban and W. Yang, *J. Membr. Sci.*, 2013, **428**, 498.
16 S. Liu, G. Liu, X. Zhao and W. Jin, *J. Membr. Sci.*, 2013, **446**, 181.
17 C. Kang, Y. Lin, Y. Huang, K. Tung, K. Chang, J. Chen, W. Hung, K. Lee and J. Lai, *J. Membr. Sci.*, 2013, **438**, 105.
18 D. Zheng, X. Liu, D. Hu, M. Li, J. Zhang, G. Zeng, Y. Zhang and Y. Sun, *RSC Adv.*, 2014, **4**, 10140.
19 I. Ahmed and S. H. Jhung, *Mater. Today*, 2014, **17**, 136.
20 O. M. Yaghi, M. O'Keeffe, N. W. Ockwig, H. K. Chae, M. Eddaoudi and J. Kim, *Nature*, 2003, **423**, 705.
21 Q. Yang, S. Vaesen, F. Ragon, A. D. Wiersum, D.Wu, A. Lago, T. Devic, C. Martineau, F. Taulelle, P. L. Llewellyn, H. Jobic, C. Zhong, C. Serre, G. D. Weireld and G. Maurin, *Angew. Chem. Int. Ed.*, 2013, **52**, 103126
22 T. Liu, L. Zou, D. Feng, Y. Chen, S. Fordham, X. Wang, Y. Liu and H. Zhou, *J. Am. Chem. Soc.*, 2014, **136**, 7813.

23 P. G. Yot, Z. Boudene, J. Macia, D. Granier, L. Vanduyfhuys, T. Verstraelen, V. Van Speybroeck, T. Devic, C. Serre, G. Férey, N. Stock and G. Maurin, *Chem. Commun.*, 2014, **50**, 9462.
24 C. Zhang, Y. Xiao, D. Liu, Q. Yang and C. Zhong, *Chem. Commun.*, 2013, **49**, 600.
25 L. Cao, K. Tao, A. Huang, C. Kong and L. Chen, *Chem. Commun.*, 2013, **49**, 8513.
26 T. Rodenas, M. van Dalen, E. García-Pérez, P. Serra-Crespo, B. Zornoza, F. Kapteijn and J. Gascon, *Adv. Funct. Mater.*, 2014, **24**, 249.
27 T. Yang and T. Chung, *J. Mater. Chem. A*, 2013, **1**, 6081.
28 T. Yang, Y. Xiao and T. Chung, *Energ. Environ. Sci.*, 2011, **4**, 4171.
29 B. Zornoza, A. Martinez-Joaristi, P. Serra-Crespo, C. Tellez, J. Coronas, J. Gascon and F. Kapteijn, *Chem. Commun.*, 2011, **47**, 9522.
30 R. Abedini, M. Omidkhah and F. Dorosti, *RSC Adv.*, 2014, **4**, 36522
31 N. A. H. M. Nordin, A. F. Ismail, A. Mustafa, R. S. Murali and T. Matsuura, *RSC Adv.*, 2014, **4**, 52530.
32 C. Zhao, N. Wang, L. Wang, H. Huang, R. Zhang, F. Yang, Y. Xie, S. Ji and J. R. Li, *Chem. Commun.*, 2014, **50**, 13921.
33 S. Sorribas, A. Kudasheva, E. Almendro, B. Zornoza, Ó. de la Iglesia, C. Téllez and J. Coronas, *Chem. Eng. Sci.*, DOI: 10.1016/j.ces.2014.07.046
34 R. Zhang, S. Ji, N. Wang, L. Wang, G. Zhang and J.-R. Li, *Angew. Chem. Int . Ed.*, 2014, **53**, 9775.
35 B. Wang, A. P. Côté, H. Furukawa, M. O'Keeffe and O. M. Yaghi, *Nature*, 2008, **453**, 207.
36 K. S. Park, Z. Ni, A. P. Cote, J. Y. Choi, R. Huang, F. J. Uribe-Romo, H. K. Chae, M. O'Keeffe and O. M. Yaghi, *Proc. Natl. Acad. Sci. U. S. A.* , 2006, **103**, 10186.
37 A. Phan, C. J. Doonan, F. J. Uribe-Romo, C. B. Knobler, M. O Keeffe and O. M. Yaghi, *Acc. Chem. Res.*, 2010, **43**, 58.
38 Y. Li, F. Liang, H. Bux, A. Feldhoff, W. Yang and J. Caro, *Angew. Chem. Int. Ed.*, 2010, **49**, 548.
39 T. Li, Y. Pan, K. Peinemann and Z. Lai, *J. Membr. Sci.*, 2013, **425-426**, 235.
40 J. Cravillon, S. Münzer, S. Lohmeier, A. Feldhoff, K. Huber and M. Wiebcke, *Chem. Mater.*, 2009, **21**, 1410.
41 W. Wei, S. Xia, G. Liu, X. Dong, W. Jin, N. Xu, *J. Membr. Sci.*, 2011, **375**, 334
42 F. Cao, C. Zhang, Y. Xiao, H. Huang, W. Zhang, D. Liu, C. Zhong, Q. Yang, Z. Yang and X. Lu, *Ind. Eng. Chem. Res.*, 2012, **51**, 11274.
43 A. G. Fadeev, M. M. Meagher, S. S. Kelley and V. V. Volkov, *J. Membr. Sci.*, 2000, **173**, 133.
44 G. Shi, H. Chen, Y. Jean and T. Chung, *Polymer*, 2013, **54**, 774
45 S. Liu, G. Liu, J. Shen and W. Jin, *Sep. Purif. Technol.*, 2014, **133**, 40
46 S. Basu, M. Maes, A. Cano-Odena, L. Alaerts, D. E. De Vos and I. F. J. Vankelecom, *J. Membr. Sci.*, 2009, **344**, 190
47 J. van den Bergh, C. Güçüyener, E.A. Pidko, E.J. M. Hensen, J. Gascon and F. Kapteijn., *Chem. Eur. J.*, 2011, **17**, 8832
48 S. Aguado, G. Bergeret, M. P. Titus, V. Moizan, C. Nieto-Draghi, N. Bats and D. Farrusseng, *New J. Chem.*, 2011, **35**, 546
49 J. Thompson, C. Blad, N. A. Brunelli, M. E. Lydon, R. P. Lively, C. W. Jones and S. Nair., *Chem. Mater.*, 2012, **24**, 1930
50 C. Kang, Y. Lin, Y. Huang, K. Tung, K. Chang, J. Chen, W. Hung, K. Lee and J. Lai, *J. Membr. Sci.*, 2013, **438**, 105.
51 S. D. Bhat and T.M. Aminabhavi, *Micropor. Mesopor. Mater.*, 2006, **91**, 206
52 X. Qiao and T. Chung, *Ind. Eng. Chem. Res.*, 2005, **44**, 8938.
53 G. Shi, T. Yang and T. Chung, *J. Membr. Sci.*, 2012, **415-416**, 577.
54 S. Amnuaypanich and P. Ratpolsan, *J. Appl. Polym. Sci.*, 2009, **113**, 3313.
55 S. Tan, L. Li, Z. Xiao, Y. Wu and Z. Zhang, *J. Membr. Sci.*, 2005, **264**, 129.
56 A. Jonquires and A. Fanes, *J. Membr. Sci.*, 1997, **125**, 245.
57 J. Huang and M. M. Meagher, *J. Membr. Sci.*, 2001, **192**, 231.
58 F. Liu, L. Liu and X. Feng, *Sep. Purif. Technol.*, 2005, **42**, 273.